Supplementary Information

Abbreviations
$[Co(4\text{-etpy})_2(hfac)_2]$ **(1)**, CCDC 2223471 (T = 100 K), this work
$[Co(4\text{-etpy})_2(hfac)_2]$ **(1c)**, CCDC 2236260 (T = 296 K), this work
$[Co(4\text{-bzpyCl})_2(hfac)_2]$ **(2)**, CCDC 2223472 (T = 100 K), this work
$[Co(acac)_2(H_2O)_2]$ (**3a**), CCDC 1842364 (T = 100 K, R_{gt} = 2.4%)
$[Co(acac)_2(H_2O)_2]$ (**3b**), CCDC 1005484 (T = 293 K, R_{gt} = 6.1%)

Two complexes under study were prepared following the synthetic route in Scheme S1. The organic reactants (4-ethylpyridine, 4-(4-chlorobenzyl)pyridine), inorganic salt cobalt(II) hexafluroacetylacetonate hydrate of reagent grade were purchase and used as received. Acetonitrile was not dried and used without any further purification.

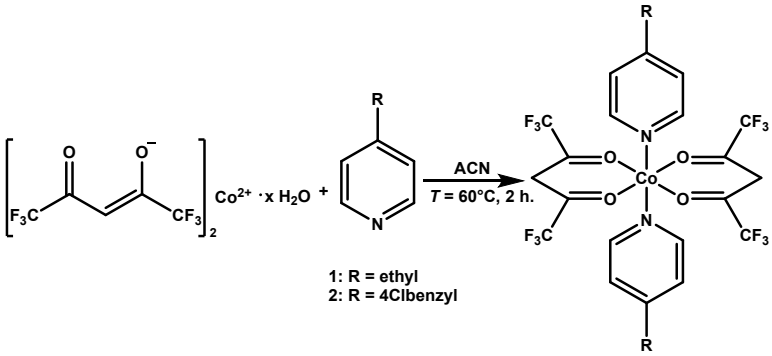

Scheme S1. Synthetic route of **1** and **2**.

Synthesis of the complex $[Co(4\text{-etpy})_2(hfac)_2]$ **(1)**.
Cobalt(II) hexafluroacetylacetonate hydrate (0.5 mmol, 0.236 g) was dissolved in acetonitrile (15 cm^3) and stirred for 15 min. Afterwards 4-etyhlpyridine (4-etpy) (1.5 mmol, 0.170 cm^3) was added. The resulting mixture was stirred and heated under reflux for 2 hours. After refluxing, the solution was filtered off and left for crystallization. The red-orange crystals were collected after 5 days. Yield: 46%. Melting point: 171°C. *Anal Calc.* for $C_{24}H_{20}CoF_{12}N_2O_4$ (M = 687.351g·mol^{-1}): C, 41.94; H, 2.93; N, 4.08. Found: C, 41.75 H, 2.82; N, 4.16. Selected IR bands / (cm^{-1}): 1641 ν_{as}(C-C), 1618 ν_s(C-O), 1251 ν_s(C-C) 1209 $\nu_{as}(CF_3)$, 1193 $\nu_s(CF_3)$ 1138 (C-H), 793 (C-CF_3). UV/Vis (Nujol) $\nu_{max}/10^3$ cm^{-1} (relat. absorb.): 27.5, 32.

Synthesis of the complex $[Co(4\text{-bzpyCl})_2(hfac)_2]$ **(2)**.
Cobalt(II) hexafluroacetylacetonate hydrate (0.5 mmol, 0.236 g) was dissolved in acetonitrile (15 cm^3) and stirred for 15 min. Afterwards 4-(4-chlorobenzyl)pyridine (4-bzpyCl) (1.5 mmol, 0.263 cm^3) was added. The resulting mixture was stirred and heated under reflux for 2 hours. After refluxing, the solution was filtered off and left for crystallization. The orange crystals were collected after 5 days. Yield: 85%. Melting point: 196°C. *Anal Calc.* for $C_{34}H_{22}Cl_2CoF_{12}N_2O_4$ (M = 880.384 g·mol^{-1}): C, 46.39; H, 2.52; N, 3.18. Found: C, 47.22 H, 2.06; N, 3.34. Selected IR bands / (cm^{-1}): 1637 ν_{as}(C-C), 1612 ν_s(C-O), 1256 ν_s(C-C), 1193 $\nu_s(CF_3)$, 1134 (C-H), 793 (C-CF_3). UV/Vis (Nujol) $\nu_{max}/10^3$ cm^{-1} (relat. Absorb.): 27.5, 32.

Note about irreducible representations for double groups with degeneracy given by the character of identity

Double groups $\mathbf{D}'_4$, $\mathbf{C}'_{4v}$, and $\mathbf{D}'_{2d}$ ($h = 16$)

Bethe symbol	Γ_1	Γ_2	Γ_3	Γ_4	Γ_5	Γ_6	Γ_7
Mulliken symbol	A_1	A_2	B_1	B_2	E_1	$E_{1/2}$	$E_{3/2}$
Griffith symbol	A_1	A_2	B_1	B_2	E	E’	E’’
Character $\chi(\hat{C}_1)$	+1	+1	+1	+1	+2	–2	–2

Double groups $\mathbf{D}'_2$ and $\mathbf{C}'_{2v}$ ($h = 8$)

Bethe symbol	Γ_1	Γ_2	Γ_3	Γ_4	Γ_5
Mulliken symbol	A/A_1	B_1/A_2	B_2/B_1	B_3/B_2	$E_{1/2}$
Griffith symbol	A/A_1	B_1/A_2	B_2/B_1	B_3/B_2	E’
Character $\chi(\hat{C}_1)$	+1	+1	+1	+1	–2

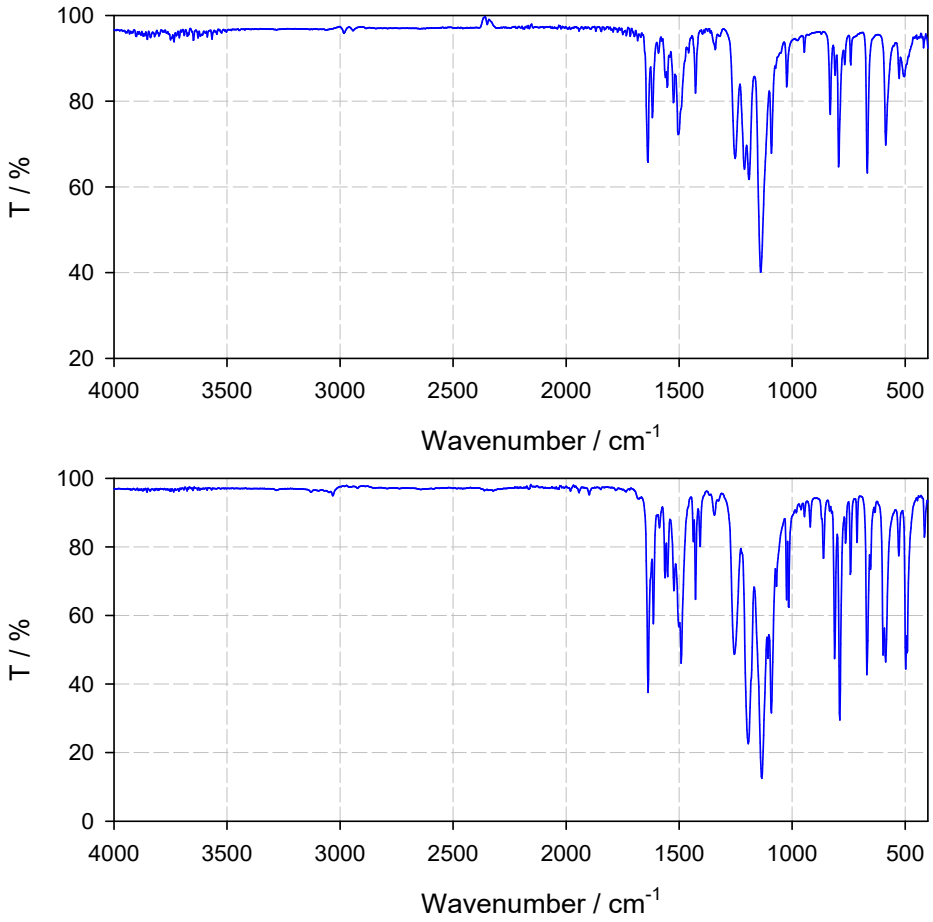

Fig. S1. IR spectra of $[Co^{II}(etpy)_2(hfac)_2]$, **1,** (top) and $[Co^{II}(bzpyCl)_2(hfac)_2]$, **2** (bottom).

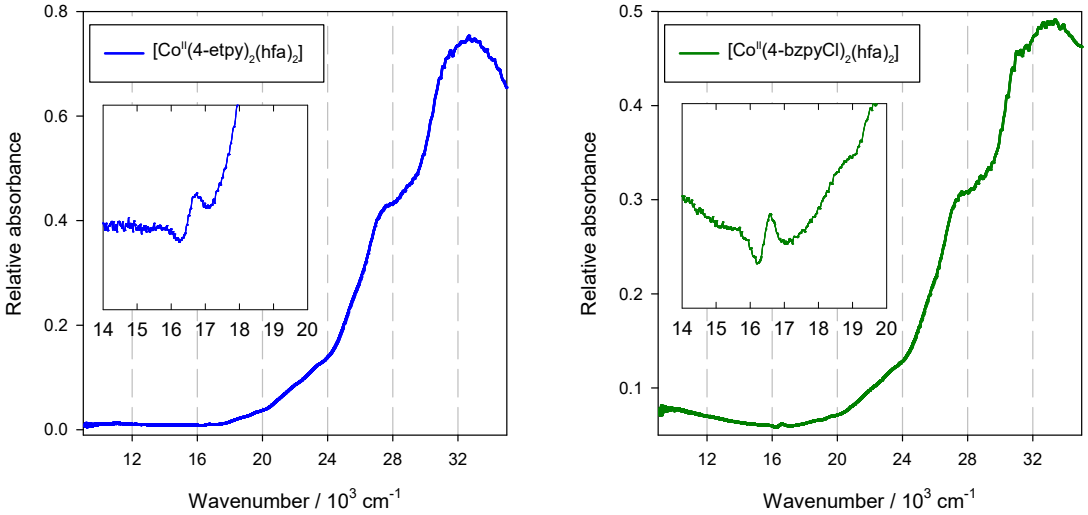

Fig. S2. Electronic spectrum of **1** and **2** in Nujol mull.
Evident electronic transitions at {$^4A_{2g}$: **16 500**}, {$^4T_{1g}$: **24 000**, 27 500}, {charge-transfer: 33 000} cm^{-1}.
Ab initio calculated quartet-to-quartet transitions for **2**: {$^4T_{1g}$(ground): 0, 300, 600}, {$^4T_{2g}$: 7400, 7900, 8300}, {$^4A_{2g}$: **16 700**}, {$^4T_{1g}$: **24 200**, 24 700, 25 100} cm^{-1}.

Table S1. Crystal data and structure refinement parameters of **1** and **2**.

	1, $[Co^{II}(etpy)_2(hfac)_2]$	**1c**, $[Co^{II}(etpy)_2(hfac)_2]$	**2**, $[Co^{II}(bzpyCl)_2(hfac)_2]$
Empirical formula	$C_{24}H_{20}CoF_{12}N_2O_4$	$C_{24}H_{20}CoF_{12}N_2O_4$	$C_{34}H_{22}Cl_2CoF_{12}N_2O_4$
Formula weight	687.351	687.351	880.384
Temperature/K	**100**	**296**	**100**
Crystal system	monoclinic	monoclinic	monoclinic
Space group	$P2_1/c$	$P2_1/c$	$P2_1/n$
a/Å	8.0773(3)	7.9911(18)	9.1173(9)
b/Å	26.4017(12)	9.202(2)	14.4277(13)
c/Å	19.7244(9)	20.709(5)	14.3485(14)
α/°	90	90	90
β/°	100.742(3)	100.335	107.966(3)
γ/°	90	90	90
Volume/Å^3	4132.6(3)	1498.2(6)	1795.4(3)
Z	6	2	2
ρ_{calc} g/cm^3	1.657	1.524	1.629
μ/mm^{-1}	5.969	0.679	0.731
F(000)	2066.90	690	884.1
Crystal size/mm^3	0.21 × 0.17 × 0.06	0.26 × 0.24 × 0.12	0.21 × 0.20 × 0.18
Radiation	Cu Kα (λ = 1.54186)	Mo Kα (λ = 0.71073)	Mo Kα (λ = 0.71073)
2Θ range /°	5.66 to 143. 68	4.0 to 50.05	4.1 to 61.2
Index ranges	$-9 \le h \le 9$, $-32 \le k \le 25$, $-17 \le l \le 24$	$-9 \le h \le 9$, $-9 \le k \le 10$, $-24 \le l \le 24$	$-12 \le h \le 13$, $-19 \le k \le 20$, $-20 \le l \le 19$
Reflections collected	47313	8689	24070
Independent reflections	7914 [R_{int} = 0.0758, R_{sigma} = 0.0650]	2643 [R_{int} = 0.0292, R_{sigma} = 0.0259]	5045 [R_{int} = 0.0337, R_{sigma} = 0.0284]
Data/restraints/parameters	7914/32/703	2643/68/223	5045/48/309
Goodness-of-fit on F2	1.036	1.089	1.051
Final R indexes [I>=2σ (I)]	R_1 = 0.0457, wR_2 = 0.0783	R_1 = 0.0506, wR_2 = 0.1421	R_1 = 0.0302 wR_2 = 0.0566
Final R indexes [all data]	R_1 = 0.0957, wR_2 = 0.0943	R_1 = 0.0661, wR_2 = 0.1548	R_1 = 0.0408 wR_2 = 0.0611
Largest diff. peak/hole / e Å^{-3}	0.59/-0.58	0.29/-0.30	0.76/-0.54
Color	Orange-red	Orange-red	Orange
CCDC No	2223471	2236260	2223472

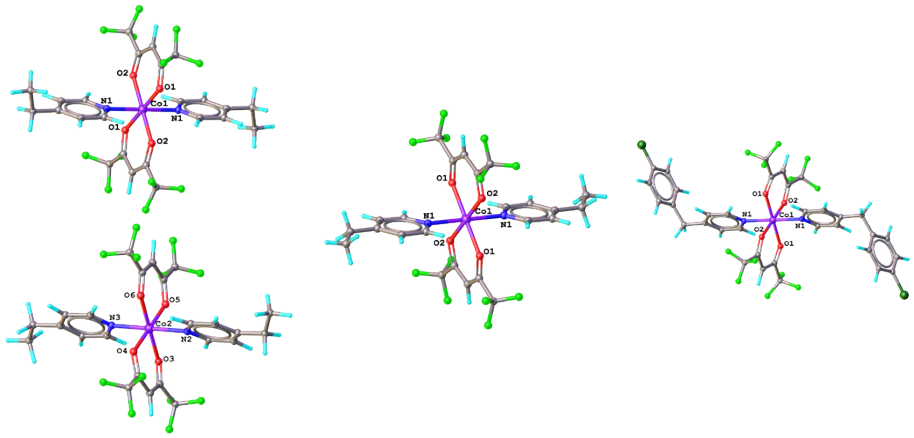

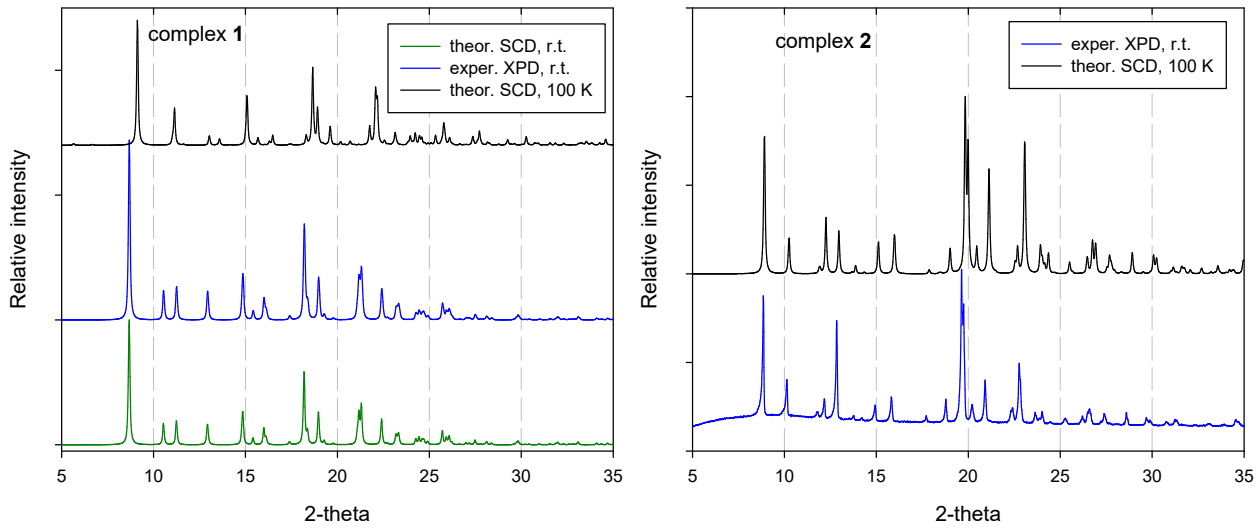

Fig. S3. Powder diffraction pattern for **1** and **2**: black – theoretical, generated from cif-files determined at T = 100 K; blue – experimental, and recorded pattern at the room temperature; red – generated form cif-file for **1** determined at the room temperature. Experimental X-ray powder diffraction (XPD) patterns for **1** measured at the room temperature match those generated from the cif-file determined by single crystal diffraction (SCD) at the room temperature; this confirms the phase identity and purity of the sample **1**. The shift of the theoretical patterns on cooling reflects the structural changes as confirmed by Table S1.

Table S2. Comparison of averaged metal-ligand distance (Å) for Co(II) complexes with shape of an elongated tetragonal bipyramid. [a]

No	Co-A ax	Co-B eq	Complex	CCDC No	Ref.
1a	Co-N 2.132	Co-O 2.052	$[Co(hfac)_2(etpy)_2]$	2223471	This work
1b	Co-N 2.151	Co-O 2.049	$[Co(hfac)_2(etpy)_2]$	2223471	This work
1c	Co-N 2.135	Co-O 2.053	$[Co(hfac)_2(etpy)_2]$	2236260	This work
2	Co-N 2.137	Co-O 2.061	$[Co(hfac)_2(bzpyCl)_2]$	2223472	This work
3a	Co-O 2.157	Co-O 2.038	$[Co(acac)_2(H_2O)_2]$	1842364	S1
3b	Co-O 2.199	Co-O 2.050	$[Co(acac)_2(H_2O)_2]$	1005484	S2
4	Co-N 2.133	Co-N 2.117	$[Co(abpt)_2(tcm)_2]$	997721	S3
5	Co-O 2.150	Co-O 2.061	$[Co^{II}Co^{III}(LH_2)_2(H_2O)(CH_3COO)]\cdot(H_2O)_3$	1440294	S4
6	Co-N 2.147	Co-O 2.113	$[Co(bz)_2(H_2O)_2(nca)_2]$	804191	S5
7	Co-O 2.113	Co-O 2.042	$[Co(H_2O)_6](OHnic)_2$	FONQUV	S6
8	Co-Cl 2.468	Co-S 2.527	$[Co(tu)_4Cl_2]$	1131921	S7

[a] Averaged distances $\bar{d}$(Co−N) = 2.185 Å, $\bar{d}$(Co−O) = 2.085 Å.

Ab initio calculations

Basis set
Co : 17s12p7d2f1g contracted to 10s7p4d2f1g pattern {8111111111/6111111/4111/11/1}
F : 7s4p1d contracted to 3s2p1d pattern {511/31/1}
O : 11s6p2d1f contracted to 6s3p2d1f pattern {611111/411/11/1}
N : 11s6p2d1f contracted to 6s3p2d1f pattern {611111/411/11/1}
C : 7s4p1d contracted to 3s2p1d pattern {511/31/1}
H : 4s contracted to 2s pattern {31}

Table S3. Results of *ab initio* calculations for $[Co(acac)_2(H_2O)_2]$. [a]

3b, $[Co(acac)_2(H_2O)_2]$, structure CCDC 1005484 at 293 K, R_{gt} = 6.1%			
CAS theory: spin-orbit multiplets and their compositions			
KD1, $N_{1,2}$ = 0.77	KD2, $N_{3,4}$ = 0.90	KD3	KD4
$\delta_{1,2}$ = 0 (ground)	$\delta_{3,4}$ = 171	$\delta_{5,6}$ = 850	$\delta_{7,8}$ = 1121
$54\cdot\lvert\pm1/2\rangle_{0,1,2}$ + $45\cdot\lvert\pm3/2\rangle_{0,1,2}$	$46\cdot\lvert\pm1/2\rangle_{0,1,2}$ + $52\cdot\lvert\pm3/2\rangle_{0,1}$	$56\cdot\lvert\pm1/2\rangle_{0,1,2}$ + $42\cdot\lvert\pm3/2\rangle_{0,1,2}$	$40\cdot\lvert\pm1/2\rangle_{0,1}$ + $57\cdot\lvert\pm3/2\rangle_{0,1}$
Approximate SH theory: score S = 68			
$^4\Delta_0$ = 0 (ground)	D = +80.2	E/D = 0.21	g_1 = 1.910
$^4\Delta_1$ **= 676**	D_1 = 44.4	E_1 = 44.4	g_2 = 2.533
$^4\Delta_2$ = 1166	D_2 = 27.3	E_2 = –27.2	g_3 = 2.863
			g_{iso} = 2.435

3a, $[Co(acac)_2(H_2O)_2]$, structure CCDC 1842364 at 100 K, R_{gt} = 2.4%			
CAS theory: spin-orbit multiplets and their compositions			
KD1, $N_{1,2}$ = 0.81	KD2, $N_{3,4}$ = 0.93	KD3	KD4
$\delta_{1,2}$ = 0 (ground)	$\delta_{3,4}$ = 155	$\delta_{5,6}$ = 915	$\delta_{7,8}$ = 1153
$53\cdot\lvert\pm1/2\rangle_{0,1,2}$ + $45\cdot\lvert\pm3/2\rangle_{0,1,2}$	$46\cdot\lvert\pm1/2\rangle_{0,1,2}$ + $52\cdot\lvert\pm3/2\rangle_{0}$	$56\cdot\lvert\pm1/2\rangle_{0,1,2}$ + $40\cdot\lvert\pm3/2\rangle_{1,2}$	$40\cdot\lvert\pm1/2\rangle_{0,1}$ + $57\cdot\lvert\pm3/2\rangle_{0,1}$
Approximate SH theory: score S = 91			
$^4\Delta_0$ = 0 (ground)	D = +72.0	E/D = 0.23	g_1 = 1.943
$^4\Delta_1$ **= 763**	D_1 = 39.7	E_1 = 39.6	g_2 = 2.462
$^4\Delta_2$ = 1398	D_2 = 22.7	E_2 = –22.8	g_3 = 2.804
			g_{iso} = 2.403

[a] Score $S = \Delta_1\cdot(\delta_{5,6} - \delta_{3,4})\cdot g_1\cdot N_{1,2}/10000$

Crystal-field calculations

This method (GCFT – Generalized Crystal-Field Theory) works in the basis set of atomic terms characterized by the angular momentum quantum numbers $\lvert I\rangle = \lvert d^n : \nu, L, M_L, S, M_S\rangle$ (ν – seniority number for repeating terms). The space covers 120 functions for a d^7 system. By applying the irreducible tensor algebra, the matrix elements of the interaction operators are evaluated: the interelectron repulsion $\hat{H}^{ee}$, crystal field $\hat{H}^{cf}$, spin-orbit coupling $\hat{H}^{so}$, Zeeman orbital and Zeeman spin interactions; their explicit forms were published elsewhere.[S8,S9,S12] The parameters dependent upon the radial functions are expressed by the Racah B and C parameters for the interelectron repulsion, and the crystal-field poles F_2(L) and F_4(L) for individual ligands L, respectively. The crystal-field pole is an individual integral for a ligand that characterizes its strength. It is

introduced as an integral over radial part of the atomic wave functions $F_k(R_L) = \left\langle \frac{r_>^k}{r_<^{k+1}} \right\rangle = \int_0^\infty R_{n,l}^*(r) \frac{r_<^k}{r_>^{k+1}} R_{n,l}(r) r^2 \mathrm{d}r \approx R_L^{-(k+1)} \cdot \left\langle r^k \right\rangle$. Then, for instance, the traditional, collective octahedral $10Dq = (10/6)F_4(R_L)$; The spin-orbit interaction is characterized by the spin-orbit coupling constant ξ_{Co}. The diagonalization of the matrix $\left\langle J \middle| \hat{H}^{ee}(B,C) + \hat{H}^{cf}(F_2,F_4) + \hat{H}^{so}(\xi) \middle| I \right\rangle$ yields the crystal-field multiplets $\left| K \right\rangle = \left| (\mathrm{d}^n \nu LS); \Gamma'_a, \gamma'_a, a \right\rangle$ where we used labeling of the irreducible representations (IRs) and their components $\{\Gamma'_a, \gamma'_a, a\}$ within the double point group of symmetry. The diagonalization matrix **U** in $E_{cm} = \mathbf{U}^+ (\mathbf{H}^{ee} + \mathbf{H}^{cf} + \mathbf{H}^{so}) \mathbf{U}$ transforms the atomic terms to the crystal-field multiplets. The complex coefficients $w_{I,K}$ (I – atomic term, K – crystal-field multiplet) are used to calculate weights in % $w_{I,K} = [\mathrm{Re}(u_{I,K})^2 + \mathrm{Im}(u_{I,K})^2] * 100$. In this way the composition of the multiplets from the spin states is evaluated, e.g. $\left| K : \Gamma', \gamma', a \right\rangle = \sum_I w_{I,K} \left| I : \nu, L, M_L, S, M_S \right\rangle$. The evaluation of the spin-Hamiltonian parameters represents an approximation based upon the construction of the **Λ**-tensor by means the 2nd-order perturbation theory $\Lambda_{ab} = \hbar^{-2} \sum_{J \neq 0} \left\langle 0 \middle| \hat{L}_a \middle| J \right\rangle \left\langle J \middle| \hat{L}_b \middle| 0 \right\rangle / (E_J - E_0)$ where the summation runs over all excited terms $\left| J \right\rangle$. The **Λ**-tensor is used in the definition of the **D**-tensor $D'_{ab} = -\lambda^2 \Lambda_{ab}$ where $\lambda = \pm\xi / 2S$ is the spin-orbit splitting parameter within the ground term having the negative sign for d^7 shells. In the traceless form $D_{ab} = D'_{ab} - \delta_{ab}(D'_{xx} + D'_{yy} + D'_{zz})/3$ the axial and rhombic zero-field splitting parameters are expressed as $D = (-D'_{xx} - D'_{yy} + 2D'_{zz})/2$ and $E = (D'_{xx} - D'_{yy})/2$.

In the GCFT calculations the key role plays an appropriate choice of the crystal field poles for individual ligands. In the present study the data selected in Table 2 were applied.

Table S4. Averaged metal-ligand distances (Å) in **2** and assigned crystal-field poles (cm^{-1}).

Average	**2**	Standard	Used F_4(L)
$\bar{d}$(Co−N) = 2.185	Co-N 2.137	F_4(N) = 6500	7300
$\bar{d}$(Co−O) = 2.085	Co-O 2.062	F_4(O) = 5500	6000
	Co-O 2.081	F_4(O) = 5500	5200

Table S5. Calculated energy levels and SH parameters by GCFT for $\{CoO_2O'_2N_2\}$ moiety.

Spin-orbit multiplets and their compositions by GCFT			
KD1	KD2	KD3	KD4
$\delta_{1,2}$ = 0 (ground)	$\delta_{3,4}$ = 184	$\delta_{5,6}$ = 652	$\delta_{7,8}$ = 967
$85 \cdot \lvert\pm1/2\rangle_{0,1,2}$ +	$11 \cdot \lvert\pm1/2\rangle_{0,1,2}$ +	$22 \cdot \lvert\pm1/2\rangle_{0,1,2}$ +	$89 \cdot \lvert\pm1/2\rangle_{0,1}$ +
$15 \cdot \lvert\pm3/2\rangle_{0,1}$	$89 \cdot \lvert\pm3/2\rangle_{0,1,2}$	$78 \cdot \lvert\pm3/2\rangle_{1,2}$	$11 \cdot \lvert\pm3/2\rangle_{0,1}$
Electronic transitions and virtual SH parameters by GCFT			
$^4\Delta_0$ = 0, $^4B_1$	D = +94	E/D = 0.18	g_1 = 2.002
$^4\Delta_1$ = 561, $^4B_2$			g_2 = 2.896
$^4\Delta_2$ = 906, $^4B_3$			g_3 = 3.300
			g_{iso} = 2.733

According to Table S5, the calculated key characteristics of the model complex are close to those obtained by *ab initio* calculations for **2**.

DC magnetic data

DC magnetic data (temperature dependence of the molar susceptibility and field fependence of the magnetization per formula unit) have been fitted simultaneously by own program MIF&FIT.[S10] The Griffith-Figgis Hamiltonian working in the space of spin-orbit kets $|L, M_L, S, M_S\rangle$ reads

$$\hat{H}^{\mathrm{GF}} = -A\kappa\lambda(\hat{\vec{L}}_{\mathrm{p}} \cdot \hat{\vec{S}})\hbar^{-2} + [\Delta_{\mathrm{ax}}(\hat{L}^2_{\mathrm{p},z} - \hat{\vec{L}}^2_{\mathrm{p}}/3) + \Delta_{\mathrm{rh}}(\hat{L}^2_{\mathrm{p},x} - \hat{L}^2_{\mathrm{p},y})]\hbar^{-2}$$
$$+\mu_{\mathrm{B}}\vec{B}\cdot(g_{\mathrm{e}}\vec{S} - A\kappa\vec{L}_{\mathrm{p}})\hbar^{-1}$$

where $A\lambda$ – spin-orbit splitting parameter modified by the Figgis CI factor A (3/2 for the weak crystal field), Δ_{ax} (Δ_{rh}) – axial (rhombic) crystal-field splitting energy, $Ag_{\mathrm{L}} = -A\kappa$ is the effective orbital magnetogyric factor (negative owing to the T-p isomorphism), κ – orbital reduction factor.[S11,S12] This formula has been extended by considering the asymmetry of the Zeeman term

$$\hat{H}_n^{\mathrm{GF}} = -A\kappa\lambda(\hat{\vec{L}}_{\mathrm{p}} \cdot \hat{\vec{S}})\hbar^{-2} + \Delta_{\mathrm{ax}}(\hat{L}^2_{\mathrm{p},z} - \hat{\vec{L}}^2_{\mathrm{p}}/3)\hbar^{-2}$$
$$+\mu_{\mathrm{B}}Bg_{\mathrm{e}}(\cos\vartheta_n\hat{S}_z + \sin\vartheta_n\hat{S}_x)\hbar^{-1}$$
$$-\mu_{\mathrm{B}}B(A\kappa_z\cos\vartheta_n\hat{L}_{\mathrm{p},z} + A\kappa_x\sin\vartheta_n\hat{L}_{\mathrm{p},x})\hbar^{-1}$$

where n is the position of the grid distributed uniformly over the polar angle θ_n. In practice, n = 11 distributed along half of the meridian secures the correct powder average for the sample with an axial character. This Hamiltonian acts to the basis set formed of twelve $|L = 1, M_L, S = 3/2, M_S>$ kets. Formally, the above Hamiltonian is isomorphous with the exchange coupled dimer possessing the axial zero-field splitting adapted for the powder average.

AC susceptibility

Temperature-frequency dependence of the AC susceptibility shows that the slow magnetic relaxation survives until T ~ 7 K.

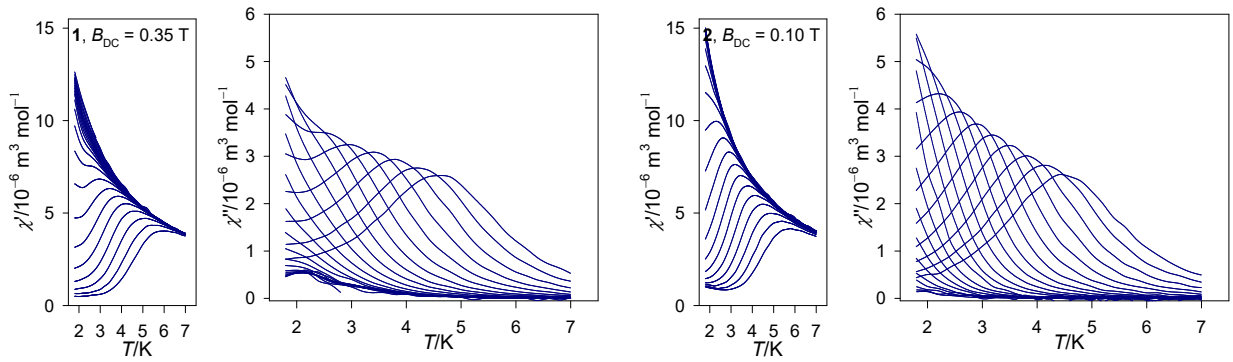

Fig. S4. Temperature-frequency dependence of the AC susceptibility for **1** and **2**.

Havriliak-Negami model (5 free parameters χ_S, χ_T, α', τ, β) is based upon the equation

$$\chi(\omega) = \chi_S + \frac{\chi_T - \chi_S}{[1 + (\mathrm{i}\omega\tau)^{\alpha'}]^{\beta}}$$

with the asymmetry parameters β and $\alpha' = 1 - \alpha$. It yields formulae for the in-phase and out-of-phase susceptibility

$$\chi'(\omega) = \chi_S + (\chi_T - \chi_S)\frac{\cos(\beta\varphi)}{[1 + 2(\omega\tau)^{\alpha'}\cos(\pi\alpha'/2) + (\omega\tau)^{2\alpha'}]^{\beta/2}}$$

$$\chi''(\omega) = (\chi_T - \chi_S)\frac{\sin(\beta\varphi)}{[1 + 2(\omega\tau)^{\alpha'}\cos(\pi\alpha'/2) + (\omega\tau)^{2\alpha'}]^{\beta/2}}$$

with

$$\varphi = \arctan\left\{\frac{(\omega\tau)^{\alpha}\sin(\pi\alpha/2)}{1 + (\omega\tau)^{\alpha}\cos(\pi\alpha/2)}\right\}$$

For β = 1 the Havriliak–Negami equation reduces to the Cole–Cole equation, for α' = 1 to the Cole–Davidson equation.[S13]

With two relaxation channels, the fitting of the AC susceptibility data is based upon an extended **Debye model**

$$\chi(\omega) = \chi_S + \frac{\chi_{T1} - \chi_S}{1 + (\mathrm{i}\omega\tau_1)^{1-\alpha_1}} + \frac{\chi_{T2} - \chi_{T1}}{1 + (\mathrm{i}\omega\tau_2)^{1-\alpha_2}} \text{ or } \chi(\omega) = \chi_S + (\chi_T - \chi_S)\left[\frac{x_1}{1 + (\mathrm{i}\omega\tau_1)^{1-\alpha_1}} + \frac{x_2}{1 + (\mathrm{i}\omega\tau_2)^{1-\alpha_2}}\right]$$

Here x_1 and x_2 are the weights of the individual relaxation channels (branches); $\omega = 2\pi f$. The parameters of the theory involve: one adiabatic susceptibility χ_S (this is a high-frequency limit), isothermal susceptibilities χ_{Tk}, distribution parameters α_k, and the relaxation times τ_k. The complex equation decomposes into two explicit formulae for

a) the in-phase component

$$\chi'(\omega) = \chi_S + (\chi_{T1} - \chi_S)\frac{1 + (\omega\tau_1)^{1-\alpha_1}\sin(\pi\alpha_1/2)}{1 + 2(\omega\tau_1)^{1-\alpha_1}\sin(\pi\alpha_1/2) + (\omega\tau_1)^{2-2\alpha_1}}$$
$$+(\chi_{T2} - \chi_{T1})\frac{1 + (\omega\tau_2)^{1-\alpha_2}\sin(\pi\alpha_2/2)}{1 + 2(\omega\tau_2)^{1-\alpha_2}\sin(\pi\alpha_2/2) + (\omega\tau_2)^{2-2\alpha_2}}$$

b) the out-of-phase component

$$\chi''(\omega) = (\chi_{T1} - \chi_S)\frac{(\omega\tau_1)^{1-\alpha_1}\cos(\pi\alpha_1/2)}{1 + 2(\omega\tau_1)^{1-\alpha_1}\sin(\pi\alpha_1/2) + (\omega\tau_1)^{2-2\alpha_1}}$$
$$+(\chi_{T2} - \chi_{T1})\frac{(\omega\tau_2)^{1-\alpha_2}\cos(\pi\alpha_2/2)}{1 + 2(\omega\tau_2)^{1-\alpha_2}\sin(\pi\alpha_2/2) + (\omega\tau_2)^{2-2\alpha_2}}$$

with the constraint for the isothermal susceptibilities $\chi_S < \chi_{T1} < \chi_{T2}$. The functional to be minimized accounts to the relative errors of both susceptibility components $F = w \cdot E(\chi') + (1-w) \cdot E(\chi'')$ with the typical weight w = 0.07, or $F = E(\chi') \cdot E(\chi'')$ with $E(\chi) = (1/N)\left[\sum_i^N \left|(\chi_i^{\mathrm{e}} - \chi_i^{\mathrm{c}})/\chi_i^{\mathrm{e}}\right|\right]$. The optimization routine refers to the genetic algorithm [D. L. Carroll, Univ. Illinois, Urbana, USA, 1998.] The quality of the fit is expressed by discrepancy factors for the in-phase and out-of phase susceptibilities $R(\chi')$ and $R(\chi'')$ defined as $R(\chi) = \sqrt{\left[\sum_i (\chi_i^{\mathrm{e}} - \chi_i^{\mathrm{c}})^2\right] / \left[\sum_i (\chi_i^{\mathrm{e}})^2\right]}$ and by the standard deviation for each optimized parameter; this is given in parentheses, e.g. 12.3(45) means 12.3 ± 4.5 (at 95% probability level). The retrieved parameters should follow a systematic trend along a smooth dependence.

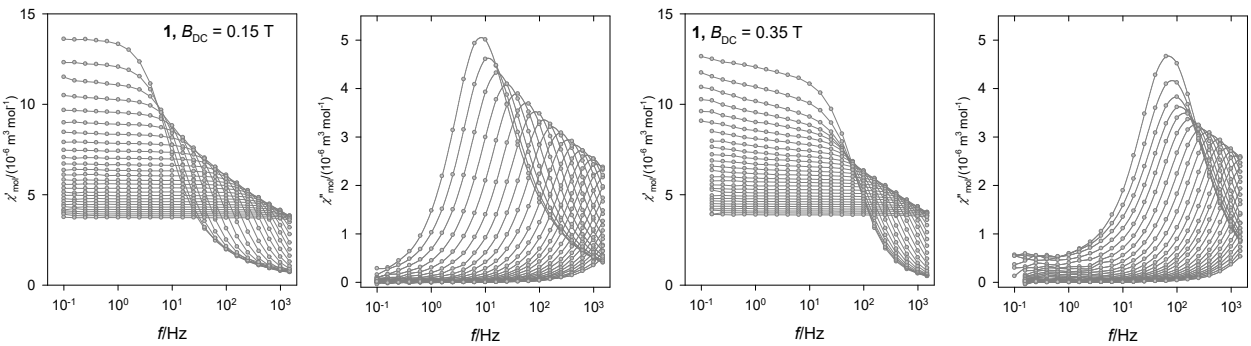

Fig. S5. Frequency-temperature dependence of the AC susceptibility for **1** at B_{DC} = 0.15 and 0.35 T.

Table S6. Parameters of the AC susceptibility for **1** at B_{DC} = 0.15 T. [a]

T/K	$R(\chi')$	$R(\chi'')$	χ_S	χ_T	α	τ/ms	β
1.8	0.3	1.0	0.66(3)	13.6(1)	.98(1)	28.6(5)	.63(1)
2.0	0.4	2.0	0.63(3)	12.5(1)	.97(1)	19.6(4)	.67(1)
2.2	0.9	1.9	0.62(4)	11.2(1)	.96(1)	12.7(4)	.72(2)
2.6	0.6	1.9	0.54(3)	9.6(1)	.97(1)	5.3(1)	.77(2)
3.0	0.7	1.7	0.43(4)	8.3(1)	.99(1)	2.36(7)	.79(2)
3.4	0.4	1.1	0.42(3)	7.4(1)	.98(1)	1.02(2)	.89(2)
4.0	0.4	1.0	0.42(5)	6.3(1)	.98(1)	0.35(1)	.98(3)
4.6	0.2	1.0	0.37(6)	5.6(1)	.98(1)	0.17(1)	.99(4)
5.2	0.2	1.3	-	4.9(1)	1.0(1)	0.10(1)	.80(10)
5.8	0.2	1.5	-	4.4(1)	.98(1)	0.047(2)	.89(4)
6.4	0.3	4.2	-	4.1(1)	.99(1)	0.032(7)	.77(15)
7.0	0.2	3.9	-	3.7(1)	.99(1)	0.033(7)	.46(9)

[a] Single-set Havriliak-Negami model. Molar susceptibilities in units of 10^{-6} m^3 mol^{-1}. $R(\chi')$ and $R(\chi'')$ – discrepancy factors of the fit.

Table S7. Parameters of the AC susceptibility for **1**. for B_{DC} = 0.25 T. [a]

T/K	$R(\chi')$	$R(\chi'')$	χ_S	χ_T(HF)	χ_T(HF)	α(HF)	τ_{HF}/ms	x_{HF}
1.8	0.3	1.2	0.25(1)	2.9(9)	14.4(9)	.13(1)	2.19(1)	.81
2.0	0.3	1.0	0.20(2)	3.5(8)	13.6(7)	.14(1)	1.88(1)	.75
2.2	0.4	1.1	0.21(3)	3.6(8)	12.9(7)	.13(1)	1.62(1)	.73
2.6	0.4	1.2	0.20(3)	2.3(5)	10.5(3)	.11(1)	1.11(1)	.80
3.0	0.3	1.1	0.17(2)	1.8(5)	9.3(4)	.09(1)	0.72(1)	.82
3.4	0.4	1.2	0.17(3)	1.3(4)	8.1(4)	.06(1)	0.44(1)	.86
4.0	0.3	1.0	0.19(2)	1.0(3)	7.0(4)	.04(1)	0.22(1)	.88
4.6	0.2	0.9	0.24(3)	0.7(3)	6.1(2)	.02(1)	0.13(1)	.93
5.2	0.6	1.5	-	0.09(9)	5.2(1)	.02(1)	0.064(1)	.98
5.8	0.2	1.0	-	0.05(2)	4.6(1)	.02(1)	0.037(1)	.99
6.4	0.1	4.4	-	0.01(1)	4.2(1)	.04(1)	0.022(1)	1
7.0	0.1	5.1	-	0.03(3)	3.9(1)	.04(1)	0.014(1)	1

[a] Two-set extended Debye model. Molar susceptibilities in units of 10^{-6} m^3 mol^{-1}.

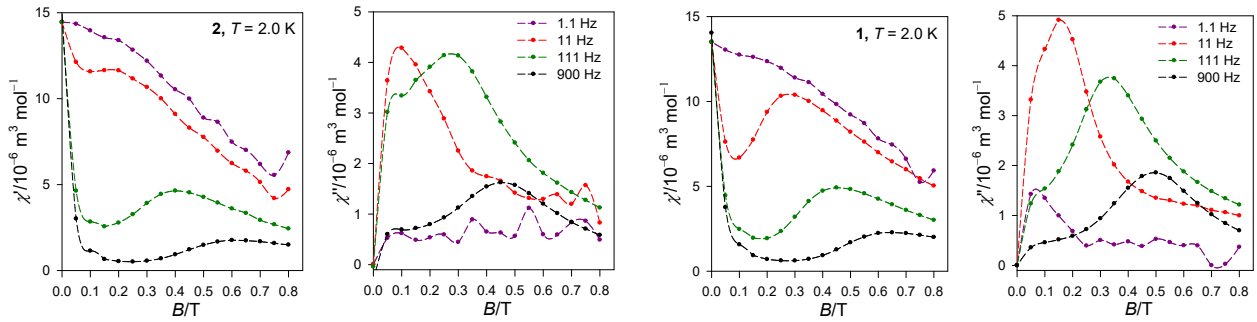

Fig. S6. Field-frequency dependence of the AC susceptibility at T = 2.0 K for **2** in comparison with **1**. Findings: there is a field supported slow magnetic relaxation.

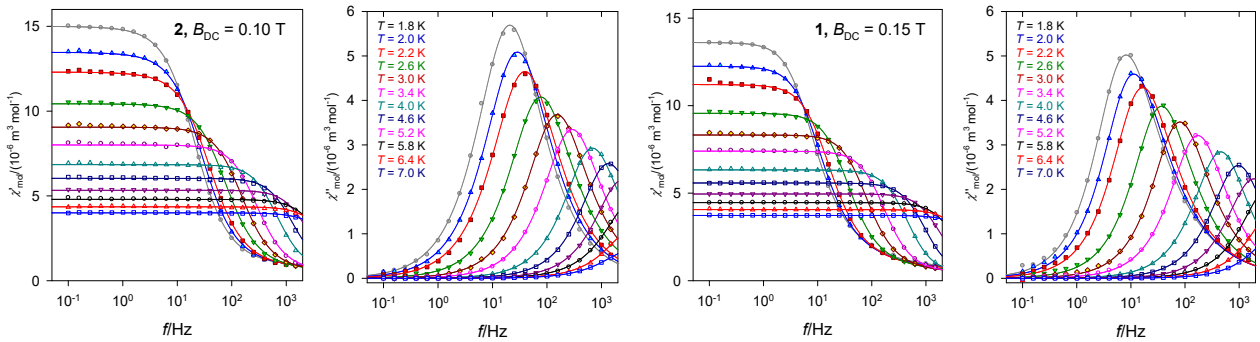

Fig. S7. Frequency-temperature dependence of the AC susceptibility for **2** in comparison with **1**.

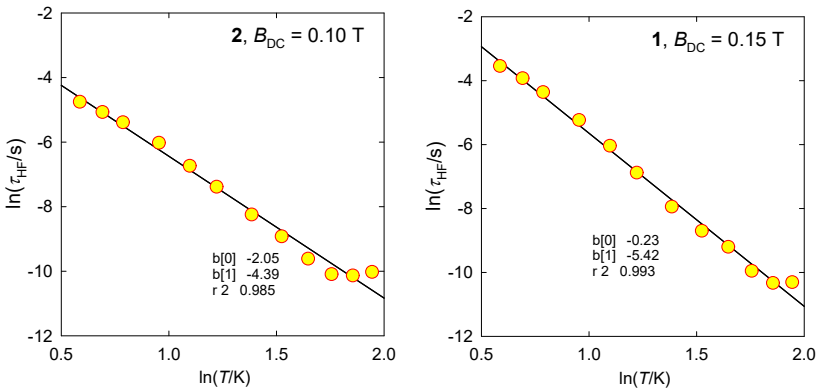

Fig. S8. Temperature dependence of the relaxation time for **2** in comparison with **1**. Straight line – regressions $\ln\tau = b_0 + b_1 \cdot \ln T$; $m = -b_1$ is the temperature coefficient in $\tau^{-1} = CT^m$.

Table S8. Parameters of the AC susceptibility for **2** at B_{DC} = 0.10 T. [a]

T/K	$R(\chi')$	$R(\chi'')$	χ_S	χ_T	α	τ/ms	β
1.8	0.34	1.7	0.80(3)	15.0(1)	0.89(1)	8.5(2)	0.89(2)
2.0	0.63	1.3	0.76(4)	13.4(1)	0.89(1)	6.2(2)	0.89(2)
2.2	0.58	1.5	0.69(4)	12.3(1)	0.89(1)	4.5(1)	0.89(2)
2.6	0.71	1.3	0.54(5)	10.4(1)	0.92(1)	2.40(8)	0.85(2)
3.0	0.82	1.1	0.48(6)	9.15(1)	0.94(1)	1.17(5)	0.86(3)
3.4	0.97	0.86	0.47(10)	8.01(1)	0.96(1)	0.61(4)	0.87(5)
4.0	1.1	1.1	0.44(23)	6.84(1)	0.98(1)	0.26(3)	0.87(10)
4.6	0.96	1.7	0.40	6.03(1)	0.98(2)	0.13(3)	0.87(23)
5.2	0.99	3.3	0.78	5.33(1)	0.98(3)	0.066(44)	1
5.8	0.89	5.6	1.0	4.79(1)	0.95(4)	0.041	1
6.4	0.78	13	2.0	4.35(1)	0.97(7)	0.039	1
7.0	0.63	11	2.6	4.00(1)	0.95(7)	0.044	1

References to SI

S1 D. H. Moseley, S. E. Stavretis, K. Thirunavukkuarasu, M. Ozerov, Y. Cheng, L. L. Daemen, J. Ludwig, Z. Lu, D. Smirnov, C. M. Brown, A. Pandey, A. J. Ramirez-Cuesta, A. C. Lamb, M. Atanasov, E. Bill, F. Neese, Z.-L. Xue, *Nature Commun.*, 2018, **9**, 2572.
S2 S. Gómez-Coca, A. Urtizberea, E. Cremades, P. J. Alonso, A. Camón, E. Ruiz, F. Luis, *Nature Commun.*, 2014, **5**, 4300.
S3 R. Herchel, L. Váhovská, I. Potočňák, Z. Trávníček. *Inorg. Chem*. 2014, **53**, 5896-5898.
S4 E. A. Buvaylo, V. N. Kokozay, O. Yu. Vassilyeva, B. W. Skelton, A. Ozarowski, J. Titiš, B. Vranovičová, R. Boča, *Inorg. Chem*. 2017, **56**, 6999−7009.
S5 J. Hudák, R. Boča, Ľ. Dlháň, J. Kožíšek, J. Moncoľ, *Polyhedron.* 2011, **30**, 1367–1373.
S6 X. L. Zhang, S. W. Ng, *Acta Cryst*. 2005, **E61**, m1140-m1141.
S7 J. E. O'Connor, E. L. Amma, *Inorganic Chemistry*, 1969, 8, 2367,
S8 R. Boča, *Struct. Bonding.* 2006, **117**, 1-260.
S9 R. Boča, R. Herchel. Program TERMS22_1.0. University of SS Cyril and Methodius, Trnava, © 2022.
S10 R. Boča, Program MIF&FIT_2.0. University of SS Cyril and Methodius, Trnava, © 2022.
S11 O. Kahn, Molecular Magnetism. VCH, Weinheim, 1993.
S12 R. Boča, A Handbook of Magnetochemical Formulae. Elsevier, Amsterdam, 2012.
S13 S. Havriliak, S. Negami, *Polymer.* 1967, **8**, 161–210.